

## EFFECT OF COOLING RATE ON THE MICROSTRUCTURE OF AN $\text{Al}_{94}\text{Mn}_2\text{Be}_2\text{Cu}_2$ ALLOY

Received – Prispjelo: 2011-07-22  
Accepted – Prihvaćeno: 2011-08-30  
Original Scientific Paper – Izvorni znanstveni rad

In this study the effect of the cooling rate on the microstructure of  $\text{Al}_{94}\text{Mn}_2\text{Be}_2\text{Cu}_2$  alloy was investigated. The vacuum induction melted and cast alloy was exposed to different cooling rates. The slowest cooling rate was achieved by the DSC ( $10 \text{ K}\cdot\text{min}^{-1}$ ), the moderate cooling rate succeeded by casting in the copper mould ( $\approx 1000 \text{ K}\cdot\text{s}^{-1}$ ) and the rapid solidification was performed by melt spinning (up to  $10^6 \text{ K}\cdot\text{s}^{-1}$ ). The microstructure of the DSC-sample consisted of  $\alpha$ -Al matrix, and several intermetallics:  $\tau_1\text{-Al}_{29}\text{Mn}_6\text{Cu}_4$ ,  $\text{Al}_4\text{Mn}$ ,  $\theta\text{-Al}_2\text{Cu}$  and  $\text{Be}_4\text{Al}(\text{Mn,Cu})$ . The microstructures of the alloy at moderate and rapid cooling consisted of the  $\alpha$ -Al matrix, i-phase and  $\theta\text{-Al}_2\text{Cu}$ . Particles of i-phase and  $\theta\text{-Al}_2\text{Cu}$  were much smaller and more uniformly distributed in melt-spun ribbons.

*Key words:* Al-alloy, metallography, microstructure, cooling rate, solidification

**Utjecaj brzne hlađenja na mikrostrukturu legure  $\text{Al}_{94}\text{Mn}_2\text{Be}_2\text{Cu}_2$ .** U ovoj je studiji istraživana utjecaj brzine hlađenja na mikrostrukturu legure  $\text{Al}_{94}\text{Mn}_2\text{Be}_2\text{Cu}_2$ . Legura sintetizirana vakuumskim indukcionim taljenjem i postupkom lijevanja bila je izložena različitim brzinama hlađenja. Najsporije je bilo hlađenje kod DSC ( $10 \text{ K}\cdot\text{min}^{-1}$ ), umjerene brzine hlađenja prilikom lijevanja u bakreni kalup ( $\approx 1000 \text{ K}\cdot\text{s}^{-1}$ ) a najviše brzine skrućivanja postignute su pomoću metode melt spinning (do  $10^6 \text{ K}\cdot\text{s}^{-1}$ ). Mikrostruktura DSC uzoraka sastoji se od matrice  $\alpha$ -Al i nekoliko intermetalnih faza:  $\tau_1\text{-Al}_{29}\text{Mn}_6\text{Cu}_4$ ,  $\text{Al}_4\text{Mn}$ ,  $\theta\text{-Al}_2\text{Cu}$  i  $\text{Be}_4\text{Al}(\text{Mn,Cu})$ . Mikrostruktura legura umjereno i brzo hlađenih sastoji se od matrice  $\alpha$ -Al, i-faze i  $\theta\text{-Al}_2\text{Cu}$ . Čestice i-faze i  $\theta\text{-Al}_2\text{Cu}$  mnogo su manje i ravnomjerno raspoređene u trakama izrađenima metodom melt spinning.

*Gljučne riječi:* Al-legura, metalografija, mikrostruktura, brzina hlađenja, skrućivanje

### INTRODUCTION

Alloys arising from the Al-Mn system contain a number of stable and metastable intermetallic phases [1]. In this system the quasicrystalline phase was reported in 1984 by Shechtman et al. [2]. Recently, Trebin et al. [3] defined a quasicrystalline state as a third solid state, in addition to crystalline and amorphous one. Atoms are regularly arranged, but they have no translational symmetry. In aluminium alloys, most of the quasicrystalline phases are thermodynamically metastable and form only under nonequilibrium conditions (about  $10^6 \text{ K}\cdot\text{s}^{-1}$ ) [4], but in some alloys they can form already at moderate cooling rates [5].

The available literature offers data about the following binary systems Al-Mn, Al-Be, Al-Cu, Be-Cu and Cu-Mn, while the Mn-Be phase diagram has not yet determined [1]. In the Al-Mn phase diagram there are several intermetallic compounds. In the aluminium corner the eutectic reaction:  $\text{L} \rightarrow \alpha\text{-Al} + \text{Al}_6\text{Mn}$  takes place at  $658 \text{ }^\circ\text{C}$  and 0,62 at.% Mn. Above the eutectic point of

the liquidus curve rises steeply:  $705 \text{ }^\circ\text{C}$  at 2,4 at. % Mn,  $765 \text{ }^\circ\text{C}$  at 5 at. % Mn.

The Al-Cu system is also a complex one with several intermetallic compounds. In the aluminium corner there is a eutectic reaction:  $\text{L} \rightarrow \alpha + \theta\text{-Al}_2\text{Cu}$ .

Among the ternary phase diagrams the systems Al-Mn-Cu and Al-Cu-Be [6] are well-studied, while only a part of the ternary system Al-Mn-Be in the aluminium corner was investigated [7]. Liquidus projection revealed four areas of primary crystallization: a solid solution of aluminium-based  $\alpha_{\text{Al}}$ ,  $\text{Al}_6\text{Mn}$ , pure beryllium ( $\alpha_{\text{Be}}$ ) and a ternary compound  $\text{Al}_{15}\text{Mn}_3\text{Be}_2$ . There are also two other possible phases  $\text{Be}_4\text{AlMn}$  and  $\mu\text{-Al}_4\text{Mn}$  [8].

In the aluminium corner of the ternary system Al-Cu-Be the following phases were identified:  $\alpha\text{-Be}$ ,  $\theta\text{-Al}_2\text{Cu}$  and  $\delta\text{-Be}_2\text{Cu}$ . According to Mondolfo [7], the structure of  $\text{Be}_4\text{AlCu}$  should be the same as the structure of  $\text{Be}_4\text{AlMn}$ . Also  $\theta\text{-Al}_2\text{Cu}$  phase can dissolve small portion of beryllium (0,8 mass %) [6].

The system Al-Mn-Cu shows particularly in the aluminium corner the complex constitution with a large number of equilibrium invariant reactions, which are mainly transitional. There are four stable intermetallic phases present:  $\text{Al}_6\text{Mn}$ ,  $\text{Al}_4\text{Mn}$ ,  $\theta\text{-Al}_2\text{Cu}$  and  $\tau_1\text{-Al}_{29}\text{Mn}_6\text{Cu}_4$ . There are no data for the systems Be-Cu-Mn and Al-Mn-Be-Cu [1,2,7,8].

T. Bončina, F. Zupanič, Faculty of Mechanical Engineering, University of Maribor, Maribor, Slovenia.

B. Markoli, Faculty of Natural Sciences and Engineering, University of Ljubljana, Ljubljana, Slovenia

In our previous work [9] we reported the development of an Al<sub>94</sub>Mn<sub>2</sub>Be<sub>2</sub>Cu<sub>2</sub> alloy having a high quasicrystalline forming ability. The main aim of this work is to investigate in detail the effect of cooling rate on the microstructure formation during solidification. Additional goal was to determine the sequence of reactions taking place during solidification.

## EXPERIMENTAL

The alloy Al<sub>94</sub>Mn<sub>2</sub>Be<sub>2</sub>Cu<sub>2</sub> was synthesized from pure Al (99,89%), Mn (99%), Cu (99,99%) and master alloy AlBe<sub>5</sub> (AFM Affilips) using vacuum induction melting and casting into bars with 50 mm diameter. The chemical composition of the synthesized alloy was determined using ICP-AES (Inductively Coupled Plasma, Atomic Emission Spectroscopy). The following composition was obtained: 90,4 wt. % Al, 4,24 wt. % Mn, 0,68 wt. % Be and 4,44 wt. % Cu.

The synthesized alloy was then cast into a permanent rectangular copper mould (100 mm × 10 mm × 1 mm) and melt-spun using a melt spinner (30M, Marko Inc). The wheel speed of the melt spinner was varied between 19,6 m/s and 25,2 m/s. DSC was performed in an STA 449 Jupiter between 100-1100 °C, with heating and cooling rates of 10 °C · min<sup>-1</sup> in pure nitrogen.

The sample preparation for the SEM (FEI, Sirion 400) and AES (Microlab 310-F) followed the standard mechanical metallographic procedures. The EDS-energy dispersive spectroscopy (Oxford INCA 350) was applied. The presence of beryllium in phases was confirmed using Auger electron spectroscopy (AES).

The X-ray diffraction (XRD) was carried out at XRD1-beamline (Elettra, Sincrotrone Trieste, Italy) using X-rays with a wavelength of 0,1 nm in a transmission mode [10].

## RESULTS AND DISCUSSION

### Microstructure and solidification of the alloy after DSC

Figure 1 shows an X-ray diffraction pattern of Al<sub>94</sub>Mn<sub>2</sub>Be<sub>2</sub>Cu<sub>2</sub> alloy after DSC. Only low angles are shown because in this range the phases with large lattice parameters, such as  $\tau_1$  and Al<sub>4</sub>Mn can be identified reliably. In addition to these phases Al<sub>2</sub>Cu and Be<sub>4</sub>Al(Mn,Cu) were also present. All these phases were also identified in the corresponding microstructure (Figure 2). Predominant phase in the microstructure was an Al-based solid solution or  $\alpha$ -Al. The fraction of Al<sub>4</sub>Mn-phase was rather low. It was usually surrounded by the  $\tau_1$ -Al<sub>29</sub>Mn<sub>6</sub>Cu<sub>4</sub>, indicating a peritectic reaction (Figure 2a). In larger interdendritic spaces,  $\theta$ -Al<sub>2</sub>Cu was present in a heterogeneous microstructural constituent resembling binary ( $\theta$ -Al<sub>2</sub>Cu +  $\alpha$ -Al) eutectic. Be<sub>4</sub>AlMn(Cu) was found in rather small amounts in the largest interdendritic spaces (Figure 2b), probably forming during the last stages of solidification.

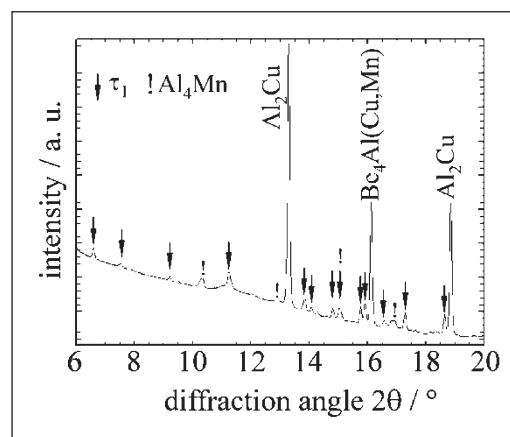


Figure 1 X-ray diffraction pattern of the alloy Al<sub>94</sub>Mn<sub>2</sub>Be<sub>2</sub>Cu<sub>2</sub> after DSC

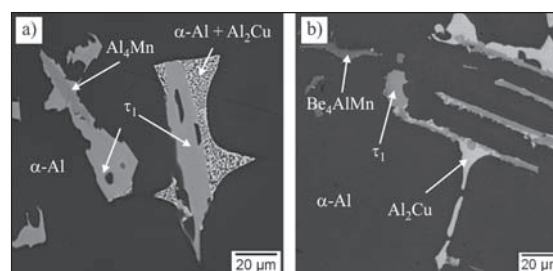


Figure 2 Backscattered electron micrographs of the alloy Al<sub>94</sub>Mn<sub>2</sub>Be<sub>2</sub>Cu<sub>2</sub> after DSC. a) A region with larger intermetallic phases, b) region, formed during the last stages of solidification

The cooling curve obtained during DSC clearly indicates the presence of three peaks, nevertheless asymmetric peaks indicate possible superposition with other smaller peaks (Figure 3). These peaks appeared at much lower temperatures than found in some Al-Mn-Be alloys. This can be attributed to the presence of Cu, and a smaller amount of Mn. It should be stressed that the peak 3 indicates that the liquidus temperature of the alloy, lies even below the melting temperature of pure Al [1].

According to the above results the following sequence of the reactions taking place during solidification can be predicted.

Primary solidification of Al<sub>4</sub>Mn begins at 654 °C (Figure 3, peak 3):



Taking into account that  $\tau_1$  completely surrounds Al<sub>4</sub>Mn, it can be reasonably concluded that a peritectic reaction takes place:



A separate peak of this reaction cannot be discerned from Figure 3. It can be supposed that this peak is superimposed with peak 2. It would not be strange because peritectic reactions are rather sluggish compared to eutectic reactions, and thus the rate of heat release is rather low.

The highest peak (peak 2) is definitely related to the formation of the Al-rich solid solution. Taking into ac-

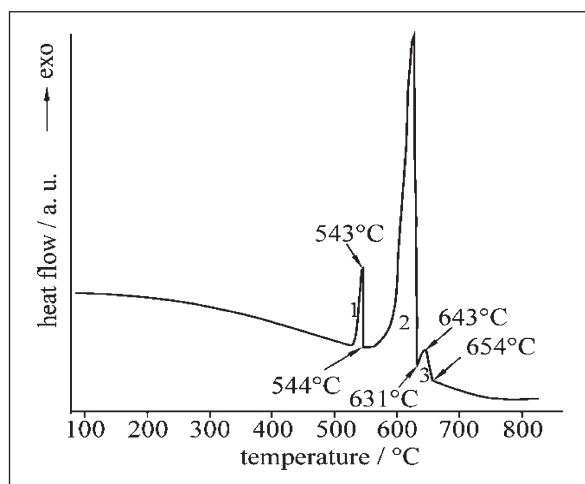


**Figure 3** Cooling curve for the alloy  $\text{Al}_{94}\text{Mn}_2\text{Be}_2\text{Cu}_2$  obtained during DSC (cooling rate  $10 \text{ K min}^{-1}$ , argon).

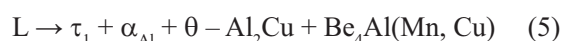
count the partition coefficients of alloying elements, which are all smaller than one, and the appearance of microstructure, it can be safely predicted that peak 2 in Figure 3 is related to the binary eutectic reaction:



In most cases solidification ceases with formation of  $\theta\text{-Al}_2\text{Cu}$ , which forms in the contact with  $\tau_1$ , thus a ternary eutectic reaction at  $544 \text{ }^\circ\text{C}$  is the most probable:



In the largest interdendritic spaces the segregation of Be to the remaining liquid exceeds its solubility, thus a Be-rich phase forms. The microstructure suggests a quaternary eutectic reaction:



In spite of rather slow cooling rates, these reactions are probably not the equilibrium ones. Nevertheless, they explain rather well the solidification microstructure.

### Solidification and microstructure of the alloy cast in a copper mould

Both XRD-pattern (Figure 4) and backscattered electron image (Figure 5) strongly indicate that only three phases  $\alpha\text{-Al}$ ,  $\theta\text{-Al}_2\text{Cu}$  and i-phase are present in the sample cooled with a moderate cooling rate. The primary i-phase was present mainly in the form of faceted particles. The symmetry of the primary i-phase already inferred their icosahedral structure.

In this sample no  $\tau_1$ ,  $\text{Al}_4\text{Mn}$  and  $\text{Be}_4\text{Al}(\text{Mn}, \text{Cu})$  were found indicating the metastable nature of microstructure. The lower tendency for forming intermetallic compounds can be already deduced from the DSC results because its liquidus temperature is lower ( $\approx 650 \text{ }^\circ\text{C}$ ) than is the typical for the two-component quasicrystalline forming alloy  $\text{Al}_{86}\text{Mn}_{14}$  ( $\approx 900 \text{ }^\circ\text{C}$ ) and alloy  $\text{Al}_{98}\text{Mn}_2$  ( $\approx 690 \text{ }^\circ\text{C}$ ) [1].

The EDS-analysis showed that it contained Al, Mn, and only around 2,5 at.% Cu. It is not possible to detect

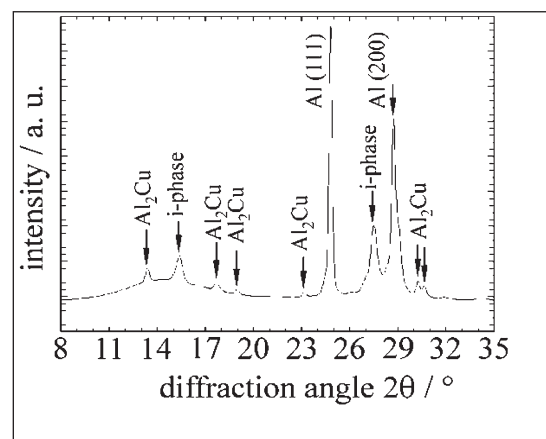


**Figure 4** X-ray diffraction pattern of the alloy  $\text{Al}_{94}\text{Mn}_2\text{Be}_2\text{Cu}_2$  after casting into the copper mould

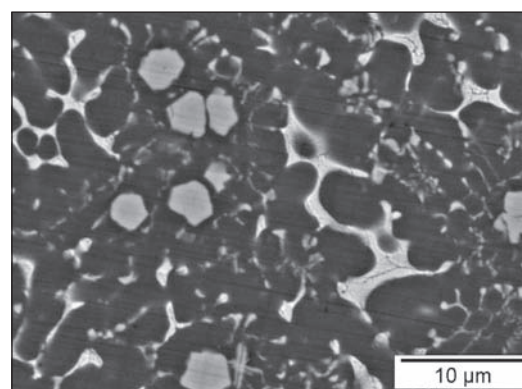


**Figure 5** BSE micrograph of the alloy  $\text{Al}_{94}\text{Mn}_2\text{Be}_2\text{Cu}_2$  cast into copper mould

Be using EDS. The i-phase was also part of two-phase eutectic cells ( $\alpha\text{-Al} + \text{i-phase}$ ). Our previous investigations clearly revealed the rodlike structure of the eutectic i-phase [11].

One can assume that beryllium atoms stabilize icosahedral clusters in the melt. Addition of copper further reduces the driving force for the formation of competing crystalline phases, and i-phase forms already at a relatively low supercooling of the melt. I-phase then grows as a primary phase exhibiting typical features of five-fold symmetry. Particles displayed mainly the shape of pentagonal dodecahedrons, and in some cases also of dendrites. The solid solution  $\alpha\text{-Al}$  afterwards nucleates on the primary particles of the i-phase. Initially it grows apparently independently of i-phase. However, at some point, mutual growth of both phases takes place, and a two-phase eutectic forms, which is designed as ( $\alpha\text{-Al} + \text{i-phase}$ ). In the remaining melt, the content of copper increases because its partition coefficient being less than one. Thus the solidification ceases with apparently a two-phase eutectic reaction  $L \rightarrow \alpha\text{-Al} + \theta\text{-Al}_2\text{Cu}$ .

### Solidification and microstructure of melt-spun ribbons

The XRD-pattern of melt-spun ribbons was apparently the same as that of the sample cast into the copper

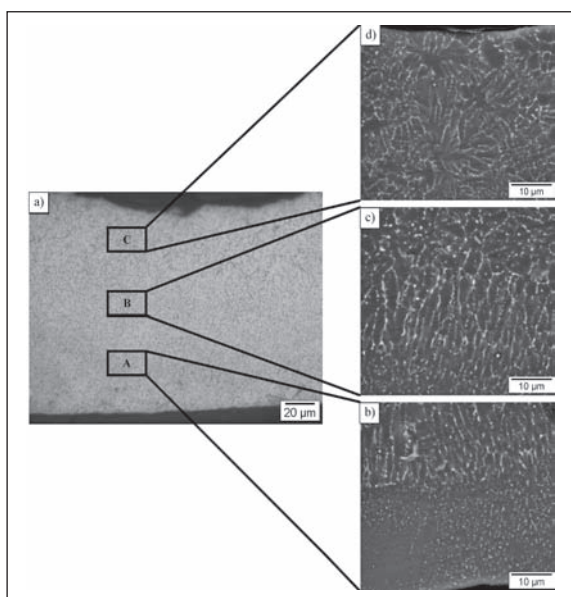


**Figure 6** Microstructure of a melt-spun ribbon of the alloy  $\text{Al}_{94}\text{Mn}_2\text{Be}_2\text{Cu}_2$ . a) Optical micrograph, b, c, d) backscattered electron micrograph of regions (A), region (B) and (C), respectively.

mould. The microstructure also consisted of matrix  $\alpha$ -Al, quasicrystalline i-phase and  $\theta$ - $\text{Al}_2\text{Cu}$  (Figure 6). The particles of i-phase and  $\text{Al}_2\text{Cu}$  were much smaller and more uniformly distributed than in the mould cast sample. The quasicrystalline particles had a circular shape, and their sizes ranged from 30 nm to 55 nm. They were mainly distributed within  $\alpha$ -Al dendrites, but some of them can also be found in the interdendritic regions. Phase  $\theta$ - $\text{Al}_2\text{Cu}$  was distributed in the interdendritic areas in the form of thin needles. Microstructure differed along the thickness of the ribbon. The smallest quasicrystalline particles were within the dendrites in region A that was in the contact with the rotating wheel. In this region  $\alpha$ -Al grew with the planar front. The quasicrystalline particles were entrapped by the solidification front, and as a result they were very uniformly distributed. In the intermediate region B directional cellular/dendritic growth took place. The diameters of the cells were only about 1 to 2  $\mu\text{m}$ . In the region C, equiaxed dendrites were present with larger distances between branches.

Solidification mechanism of the melt-spun sample can be as follows: (a) Particles with the icosahedral symmetry form in the supercooled melt, and start to grow. (b) Heterogeneous nucleation of  $\alpha$ -Al occurs on the wheel, and it grows with the planar front, which captures the icosahedral particles present in the melt. (c) Crystallization heat causes recalescence, thus many icosahedral particles in the melt disappear, and the shape of the liquid-solid solidification front turns to cellular-

dendritic one. (d) Survived icosahedral particles start to grow and some petal-like particles appeared. In e) further growth of icosahedral particles takes place, finally causing the formation of equiaxed dendrites of  $\alpha$ -Al.

## CONCLUSIONS

The results of the present investigation lead us to the following conclusions:

The microstructure of the DSC-sample that was exposed to such small cooling rate as  $10 \text{ K min}^{-1}$  consisted of  $\alpha$ -Al matrix, and several intermetallic phases:  $\tau_1$ - $\text{Al}_{29}\text{Mn}_6\text{Cu}_4$ ,  $\text{Al}_4\text{Mn}$ ,  $\theta$ - $\text{Al}_2\text{Cu}$  and  $\text{Be}_4\text{Al}(\text{Mn,Cu})$ .

Increasing cooling rates prevented the formation of  $\tau_1$ - $\text{Al}_{29}\text{Mn}_6\text{Cu}_4$ ,  $\text{Al}_4\text{Mn}$  and  $\text{Be}_4\text{Al}(\text{Mn,Cu})$ . Instead, an icosahedral quasicrystalline phase (i-phase) formed. Thus the microstructure of the alloy at moderate and rapid cooling consisted of the  $\alpha$ -Al matrix, i-phase and  $\theta$ - $\text{Al}_2\text{Cu}$ . Particles of i-phase and  $\alpha$ - $\text{Al}_2\text{Cu}$  were much smaller and more uniformly distributed in melt-spun ribbons.

Microstructural analyses of the sample cooled at different cooling rates allowed us to propose possible solidification sequences.

## REFERENCES

- [1] T.B. Massalski, H. Okamoto, P.R. Subramanian, L. Kasperzak, Binary Alloys Phase Diagrams, 2<sup>nd</sup> edition, ASM Metals Park Ohio 1990.
- [2] D.S. Shechtman, I. Blech, D. Gratias, J.W. Cahn, *Phy.Rev. Lett.*, 53 (1984), 1951-1953.
- [3] Quasicrystals, Structure and Physical Properties. Ed. H.R. Trebin, Wiley-VCH GmbH & Co. KgaA, Weinheim 2003.
- [4] W. Steurer, S. Deloudia, *Acta Crystallographica Section A*, 64 (2008), 1-11.
- [5] G.S. Song, E. Fleury, S.H. Kim, W.T. Kim, D.H. Kim, *Journal of Alloys and Compounds*, 342 (2002), 251-255.
- [6] Ternary Alloys. Ed. G. Petzow and G. Effenberg, VCH Verlagsgesellschaft, Weinheim, Basel (Switzerland); Cambridge; New York, 1988.
- [7] L.F. Mondolfo, Aluminum alloys, Structure and Properties, Butterworths, London, Boston, Sydney, Wellington, Durban, Toronto 1976.
- [8] B. Markoli, T. Bončina, F. Zupanič, *Croatica Chemica Acta*, 83 (2010) 1, 49-54.
- [9] F. Zupanič, T. Bončina, N. Rozman, I. Anžel, W. Grogger, C. Gspan, F. Hofer, B. Markoli, *Z. Kristallogr.* 223 (2008), 735-738.
- [10] S. Bernstorff, E. Busetto, C. Gramaccioni, A. Lausi, L. Olivi, F. Zanini, A. Savoia, M. Colapietro, G. Portalone, M. Camalli, A. Pifferi, R. Spagna, L. Barba, A. Cassetta, *Review of scientific instruments*, 66 (1995), 1661-1664.

**Note:** Responsible for English language is Paul J. McGuinness, Ph.D., Institute Josef Stefan Ljubljana, Slovenia.